BOUND-FREE PAIR PRODUCTION MECHANISM AT THE NICA ACCELERATOR COMPLEX*

Melek Yilmaz Şengül

Atakent Mahallesi, 3.Etap, 34303 Halkalı-Küçükçekmece İstanbul, Turkey
melekaurora@yahoo.com

(Received December 29, 2020; accepted August 25, 2021)

In this work, the bound-free pair production (BFPP) cross-section calculations are done for NICA collider. In the BFPP mechanisms, after free pair production process, free electron is captured by one of the ions. This causes the decrement of the ion from the beam, and also diminish the intensity of the beam and changes the beam lifetime. The BFPP cross-section calculations are done for the p–Au and p–Bi collisions for NICA collider which are performed in the range of a few mbarns. In this work, we used the lowest-order perturbation theory and our calculations are done in the QED framework.

DOI:10.5506/APhysPolB.52.1233

1. Introduction

In this work, we have studied the bound-free electron–positron pair production mechanism in which electron is captured by the colliding ions

$$Z_x + Z_y \to (Z_x + e^-)_{1s_{1/2}} + Z_y + e^+ \,. \tag{1}$$

This mechanism is important in the collisions of heavy ions. The BFPP cross section at RHIC and LHC energy levels is in the range of hundreds of barns and is smaller than the free pair production cross section. However, the calculation of this cross-section process is significant for the detection of the reducement of the beam intensity and this process leads to a separate beam of one-electron ions that impinges the beam pipe about 140 m away from the interaction point [1–10].

The Nuclotron-based Ion Collider fAcility (NICA) Project is in the improvement process at JINR (Dubna). The main aims of the NICA project are to supply colliding beams for experimental studies of both hot and dense strongly interacting baryonic matter and spin physics. The first program will include the running of heavy-ion mode in the energy interval of $\sqrt{s_{NN}} = 4$–11 GeV for Au nuclei. At this stage of the project, firstly the fixed target experiments with the heavy-ion beam will be deducted from the Nuclotron at kinetic energies up to 4,5 GeV/u. The polarized beam mode is aimed to be studied in the energy interval of $\sqrt{s_{NN}} = 12$–27 GeV (protons). The detailed information about the NICA can be found in [11].

The aim of this work is to investigate and examine the importance of the BFPP mechanism at NICA collider which is under construction. We will consider the proton–nucleus collision with the proton energy up to 12 GeV. To give reliable contributions to the future experiment at NICA collider, we applied our previous BFPP mechanism calculations to the proton–ion collisions that worked well when we compared our cross-section results with [12].

In Section 2, we give the detailed information about how we applied our BFPP mechanism calculations for the proton–nucleus collisions of the NICA collider parameters.

In Section 3, we give our proton–nucleus collisions cross-section results for the NICA collider and compared our calculations with [12].

We concluded in Section 4.

2. Formalism

In this study, we have calculated the BFPP cross section of the proton–ion collision for NICA collider. We did our calculations by using the semi-classical approximation and reached the exact results by using the Monte Carlo method. We obtained the BFPP cross section in the framework of QED with the help of the lowest-order perturbation theory. Detailed calculations about the BFPP cross-section process can be examined in our previous papers [9, 13, 14].

In our previous works, we used the symmetric collisions. However, our method can be implemented to asymmetric collisions such as proton–ion collisions. The colliding proton energy is 10 GeV, and it is comparable with the Au and Bi and the rest masses of the proton and nucleon are not very significant and this justifies applying the system in the center of momentum frame. The detail formulation can be found in [13].

We did our calculations by using the semi-classical approximation and we assumed that the positron goes on a straight way. We used the Sommerfeld–Maue wave-function for the positron

$$\Psi_q^{(+)} = N_+ \left[\mathrm{e}^{i\boldsymbol{q}\cdot\boldsymbol{r}}\, \boldsymbol{u}_{\sigma_q}^{(+)} \right] , \qquad (2)$$

where $\boldsymbol{u}_{\sigma_q}^{(+)}$ shows the spinor structure.

For the representation of the electron, we used the Darwin wave-function

$$\Psi^{(-)}(\vec{r}) = \left(1 - \frac{i}{2m}\,\vec{\alpha}\cdot\vec{\nabla}\right) \boldsymbol{u}\frac{1}{\sqrt{\pi}} \left(\frac{Z}{a_H}\right)^{3/2} \mathrm{e}^{-Zr/a_H} . \tag{3}$$

Using the above wave-functions, the direct Feynman diagram can be presented as

$$\left\langle \Psi^{(-)} \left|\chi_{pi}\right| \Psi_q^{(+)} \right\rangle = \frac{iN_+}{2\beta} \frac{1}{\sqrt{\pi}} \left(\frac{Z}{a_H}\right)^{3/2} \int \frac{\mathrm{d}^2 p_\perp}{(2\pi)^2} \,\mathrm{e}^{i\left(\boldsymbol{p}_\perp - \frac{\boldsymbol{q}_\perp}{2}\right)\cdot \boldsymbol{b}}\, C(\boldsymbol{p}_\perp, \boldsymbol{k}_\perp, \beta) , \tag{4}$$

where b represents the impact parameter of the proton–ion collision, and $C(\boldsymbol{p}_\perp, \boldsymbol{k}_\perp, \beta)$ function expresses the scalar part of the field correlated with the ion i and the proton p in the momentum space and transverse momentum components. Detailed information about these functions can be found in [9, 13, 14].

Using the amplitudes for the direct χ_{pi} and crossed χ_{ip} diagram, the BFPP cross section in collisions of the proton–ion collision can be expressed as

$$\sigma_{\mathrm{BFPP}} = \int \mathrm{d}^2 b \sum_{q<0} \left| \left\langle \Psi^{(-)} \left|\chi_{pi} + \chi_{ip}\right| \Psi_q^{(+)} \right\rangle \right|^2 , \tag{5}$$

that are the direct and crossed terms summation. These calculations have been accomplished for the BFPP cross sections in relativistic collisions of the proton–ion collision.

For the symmetric heavy-ion collisions with charge Z, the BFPP cross-section results increase with $\sigma_{\mathrm{BFPP}} \approx (Z\alpha)^8 \ln(\gamma)$. The behaviour of the BFPP cross-section changes as $\sigma_{\mathrm{BFPP}} \approx (Z_i\alpha)^6 (Z_p\alpha)^2 \ln(\gamma)$ in proton–ion collisions, where Z_i expresses the heavy ion and Z_p expresses the projectile proton.

3. Results and discussions

p–Au and p–Bi collisions cross-section results are seen in Fig. 1. The BFPP cross-section results in p–Au and p–Bi collisions with proton energy of 10 GeV and the ion energy of 5 GeV/nucleon ($\gamma = 100$) at NICA collider are equal to 6,5 mbarn and 8,7 mbarn in our work, respectively. These BFPP cross-section results in p–Au and p–Bi collisions at NICA collider obtained in [12] are approximately equal to 4,5 mbarn and 6 mbarn, respectively. When we compare our BFPP cross-section results for p–Au and p–Bi collisions at the NICA collider with these obtained in [12], it can be seen that our cross-section results are approximately 40% higher than those in [12]. In [12], to calculate the p–Au and p–Bi collisions cross-section results, equivalent photon approximation is used with the modification of the Sauter approximation. Modifications are done for the NICA energy region. At lower energies and the asymmetric collisions, Eq. (17) given in [12] does not work. In [12], new approximation is calculated for NICA collisions and its asymptotic form is identical to Eq. (17) given in [12]. The advantage of our method is that we can use our approximate BFPP cross-section expression for the lower energy of the colliding nuclei and also to the asymmetric collision as proton–nucleus.

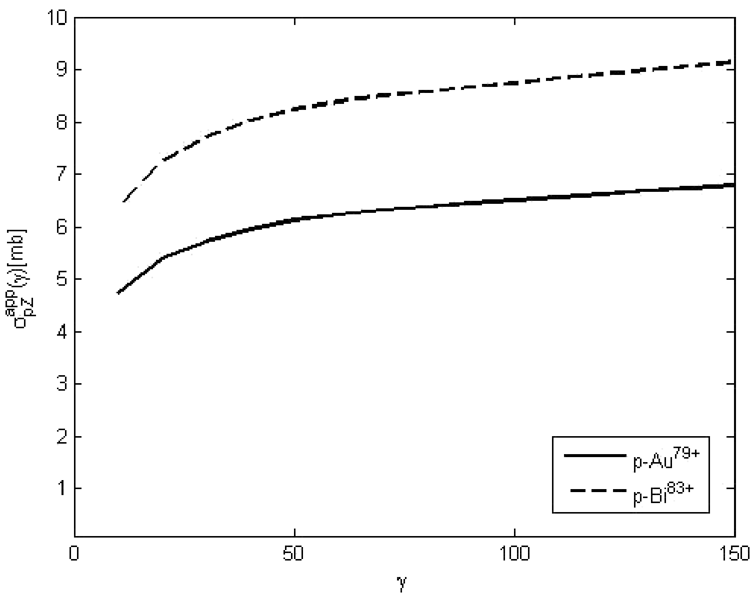

Fig. 1. Cross sections (mbarn) for p–Au and p–Bi collisions dependent on γ.

In Fig. 1, we showed the cross sections for p–Au and p–Bi collisions dependent on γ. The behaviour of our graph is similar to that of the graph in Fig. 4 given in [12]. However, our cross-section results are a few mbarn higher than those obtained in [12]. The reason for the difference can be explained as follows: we used the more general cross-section formula that can be applied in every energy range and also the asymmetric collisions.

We reached the BFPP cross-section results in the center-of-momentum frame. $\gamma = 1/\sqrt{1-v^2} = E/m_0$ is the relationship between γ (Lorentz factor) and the collider energy per nucleon E/A which is in GeV unit. In this equation m_0 represents the mass of the nucleons.

4. Conclusions

In the present paper, we did the BFPP cross-section calculations for NICA collider. The BFPP cross-section results for p–Au and p–Bi collisions with the ion energy of 5 GeV/nucleon and the proton energy of 10 GeV are in the order of magnitude of 6–8 mbarn at NICA collider. We also compared our cross-section value with the cross-section value obtained in [12]. The results are close to each other. The BFPP process leads to a decrease in the intensity of colliding beams. On the other hand, in this work, the calculated cross-section results are much smaller than the cross-section results reached for hadronic interactions, and as a result there is no decrease in the intensity of colliding beams. In our calculations, we did not add the effects of the excited atomic states to the capture cross-section results that change approximately by 10%. Also, with the cross-section calculation of p–ion collisions, we hope to give contribution to the new building of NICA collider.

REFERENCES

[1] C.A. Bertulani, G. Baur, «Electromagnetic processes in relativistic heavy ion collisions», *Phys. Rep.* **163**, 299 (1988).

[2] H. Meier *et al.*, «Bound-free electron–positron pair production in relativistic heavy-ion collisions», *Phys. Rev. A* **63**, 032713 (2001).

[3] A.J. Baltz, M.J. Rhoades-Brown, J. Weneser, «Heavy-ion partial beam lifetimes due to Coulomb induced processes», *Phys. Rev. E* **54**, 4233 (1996).

[4] A.J. Baltz *et al.*, «The physics of ultraperipheral collisions at the LHC», *Phys. Rep.* **458**, 1 (2008).

[5] C.A. Bertulani, D. Dolci, «Pair production with electron capture in peripheral collisions of relativistic heavy ions», *Nucl. Phys. A* **683**, 635 (2001).

[6] M.J. Rhoades-Brown, C. Bottcher, M.R. Strayer, «Feynman Monte Carlo calculations of electron capture at relativistic collider energies», *Phys. Rev. A* **40**, 2831 (1989).

[7] M.J. Rhoades-Brown, C. Bottcher, M.R. Strayer, «Convergence of bound-electron–positron pair production calculations for relativistic heavy-ion collisions», *Phys. Rev. A* **50**, 4842 (1994).

[8] A. Aste, K. Hencken, D. Trautmann, G. Baur, «Electromagnetic pair production with capture», *Phys. Rev. A* **50**, 3980 (1994).

[9] M.Y. Şengül, M.C. Güçlü, S. Fritzsche, «Bound-free electron–positron pair production in relativistic heavy-ion collisions», *Phys. Rev. A* **80**, 042711 (2009).

[10] M.Y. Şengül, M.C. Güçlü, «Bound free electron–positron pair production accompanied by giant dipole resonances», *Phys. Rev. C* **83**, 014902 (2011).

[11] V.D. Kekelidze *et al.*, «Three stages of the NICA accelerator complex», *Eur. Phys. J. A* **52**, 211 (2016).

[12] D.A. Bauer, D.V. Karlovets, V.G. Serbo, «Bound-free pair production in relativistic nuclear collisions from the NICA to the HE LHC colliders», *Eur. Phys. J. A* **56**, 200 (2020).

[13] M.Y. Şengül, «Bound-free electron–positron pair production mechanism at an electron–ion collider», *Int. J. Mod. Phys. E* **26**, 1750055 (2017).

[14] M.Y. Şengül, M.C. Güçlü, «Relativistic antihydrogen production by pair production with positron capture», *Prog. Part. Nucl. Phys.* **67**, 612 (2012).